Colloid Polym Sci (2007) 285:621–630
DOI 10.1007/s00396-006-1579-3

ORIGINAL CONTRIBUTION

Preparation of polysaccharide-coated nanoparticles by emulsion polymerization of styrene

C. Ladaviere · M.-C. Averlant-Petit · O. Fabre · A. Durand · E. Dellacherie · E. Marie

Received: 2 June 2006 / Accepted: 4 September 2006 / Published online: 19 January 2007

Abstract It is the aim of this paper to describe the preparation of polysaccharide-coated nanoparticles by direct emulsion polymerization of styrene in the presence of native dextran. In spite of the lack of surface-active properties of native dextran, stable latexes with very low amount of coagulate were obtained. Particle size decreased with dextran concentration and molecular weight. The amount of permanently adsorbed dextran was determined by direct titration of the polysaccharide present on the surface of the nanoparticles. A maximum value of 2.5 mg m^{-2} was found. Zeta-potential measurements allowed us to estimate the thickness of the hydrophilic layer, which regularly increased with dextran aqueous concentration. The dextran-coated polystyrene nanoparticles were stable in concentrated NaCl solutions and could be redispersed after freeze-drying. The mechanism of chemical modification of dextran was studied by nuclear magnetic resonance and matrix-assisted laser desorption/ionization-time of flight spectrometry studies. Graft copolymers are supposed to be formed.

C. Ladaviere
Systèmes Macromoléculaires et Physiopathologie Humaine,
UMR CNRS-Biomérieux 2714,
Ecole normale supérieure de Lyon, 46, Allée d'Italie,
69007 Lyon, France

M.-C. Averlant-Petit · O. Fabre · A. Durand · E. Dellacherie · E. Marie (✉)
Laboratoire de Chimie Physique Macromoléculaire,
UMR CNRS-INPL 7568,
Groupe ENSIC, BP 20451,
54001 Nancy Cedex, France
e-mail: Emmanuelle.Marie@ensic.inpl-nancy.fr

Keywords Polysaccharide · Emulsion polymerization · In situ modification

Introduction

In recent years, voluminous research has been carried out in nanoengineering and design of nanometric materials with tailored properties. In particular, polymeric nanoparticles with controlled surface properties have been increasingly used as tools in studies of colloidal models and in a variety of applications: adhesive technology and coating, drug delivery systems, medical diagnostic tests, separation media, etc. Among these particles, polysaccharide-coated nanoparticles and nanodroplets are very attractive candidates particularly for biomedical applications since polysaccharides are natural polymers exhibiting biocompatibility. Our laboratory has been developing the synthesis of polysaccharide-covered nanoparticles for about 15 years. Several processes were followed: direct adsorption of amphiphilic polysaccharides onto preformed polymeric nanoparticles and emulsion preparation followed by solvent evaporation using amphiphilic polysaccharides as polymeric emulsifiers [1–5]. More recently, polysaccharide-covered nanoparticles were prepared by miniemulsion radical polymerization stabilized by amphiphilic derivatives of dextran [6, 7]. However, these techniques require a chemical modification of the polysaccharide before particle formation because native polysaccharide exhibits poor surface-active properties [8–11].

Some studies report on emulsion polymerization in the presence of native dextran despite its lack of surface-active properties. Authors assumed that chemical modi-

fication of dextran leading to in situ formation of surface-active species occurred in the aqueous phase, thereby allowing the emulsion polymerization [10]. The mechanism of in situ formation of this biocompatible stabilizer seems to depend mainly on the initiator used. In the case of polymerization initiated by Cerium IV ions in acidic medium [12–17], the polysaccharidic chains are cleaved, leading to several dextran macro-radicals. Polymerization is initiated by the polysaccharide radicals, and block copolymers are formed. These copolymers spontaneously formed nanoparticles. The structure of these block copolymers (di-block, tri-blocks, etc.) is still under debate. When the polymerization is initiated by potassium persulfate (KPS) or peroxide derivatives [12, 18–24], graft copolymers are supposed to be formed via a hydrogen abstraction mechanism. Amphiphilic species are formed, which stabilize the emulsion polymerization of the monomer. However, no clear evidence of this later phenomenon was given.

The understanding of mechanism of the chemical modification of dextran is of particular interest to control the final properties of the latex (amount of grafted polysaccharide, colloidal stability of the latexes, etc.). Furthermore, in situ formation of polymeric stabilizers has recently gained new interests, especially in the field of controlled radical polymerization [25–30]. In that case, the aim is mainly to overcome the problems reported for controlled radical polymerization in dispersed media (poor colloidal stability, poor molecular weight control, etc.).

This paper describes the preparation of polysaccharide-coated nanoparticles by direct emulsion polymerization of styrene in the presence of native dextran. In spite of the lack of surface-active properties of native dextran, stable particles with a permanently grafted dextran layer at their surface were obtained. The amount of coagulate was very low despite the quite high solid content (10 wt.%) as compared to the usual soap-free emulsion polymerization solid content. Dextran concentration and molar masses were varied to depict their influence onto the final particle size. The particles formed were carefully analyzed, and the amount of adsorbed polysaccharide and the thickness of the hydrophilic layer were determined. This leads to a complete description of the emulsion polymerization of styrene initiated by KPS and stabilized by dextran. Finally, an important part of the present study is devoted to an investigation into the mechanism of chemical modification of dextran during emulsion polymerization of styrene initiated by KPS. Fundamental investigations have been performed by means of nuclear magnetic resonance (NMR) spectroscopy and matrix-assisted laser desorption-ionization time-of-flight mass spectrometer (MALDI TOF MS) analysis to assess the nature of the polysaccharidic species formed.

Experimental

Materials

The three dextrans T6, T40, and T500, obtained from Pharmacia (Uppsala, Sweden), have been characterized by size exclusion chromatography/multi-angle laser light scattering (SEC–MALLS) in $NaNO_3$ 0.1 M (Table 1).

Their molar masses were $\overline{M_w} = 6,430,\ 40,000,$ and $480,000\ g\ mol^{-1}$, respectively.

The other chemicals were purchased from Aldrich (St Quentin Fallavier, France). Styrene was distilled under reduced pressure before use. The other chemicals were used as received. MilliQ Water was used for all the experiments.

Emulsion polymerization of styrene

To ensure a complete dissolution of the polysaccharide, the dextran T6, T40, or T500 was first dissolved in MilliQ water for 2 h. Styrene was then added to the solution and potassium persulfate (KPS: $K_2S_2O_8$) or azobis-isobutyronitrile (AIBN) were used as initiator. The volume fraction of the organic phase was varied between 5 and 20 vol.%, while the molar fraction [KPS] / [styrene] was kept constant (0.65 mol%). At this stage, no emulsion was formed. The polymerization was performed at 75 °C under magnetic stirring (stirring rate 600 rpm). Starting from the aqueous solution of dextran and KPS topped by a styrene layer, stable latexes with very low amount of coagulate (<5 wt.%) were obtained after 12 h. Final conversion attained 96 wt.%.

When needed, samples were removed at frequent intervals and quenched by adding hydroquinone followed by rapid cooling in an ice/water mixture. The samples were purified by dialysis against ethanol/water 80/20 mixtures then water, and finally freeze-dried.

Size measurements of latex particles

Particle sizes were measured by dynamic light scattering at low concentration using an HPPS-ET instrument from Malvern. Although this apparatus is able to measure relatively concentrated samples, the latexes were diluted in pure water. Indeed, dilution in water, 10^{-3} mol l^{-1} NaCl, or polymer solution gave the same result.

Table 1 Molar masses of the dextrans T6, T40, and T500 as measured by SEC–MALLS in $NaNO_3$ 0.1 M

Dextran	T6	T40	T500
$\overline{M_n}(g\ mol^{-1})$	4,260	26,000	289,700
$\overline{M_w}(g\ mol^{-1})$	6,430	40,000	480,000
I_p	1.5	1.6	1.6

Scanning electron microscopy pictures were obtained with a Jeol JSM T330A apparatus. The samples were coated with gold before examination.

Surface properties of the particles

The amount of dextran at the particle surface after polymerization was calculated from the difference between the initial dextran amount and that remaining in the aqueous solutions after particle removal via centrifugation. Dextran concentration in the aqueous phase was determined by spectroscopy via the anthrone method [2, 31].

The styrene particles were washed via centrifugation and redispersion in distilled water to eliminate the non-adsorbed polysaccharide. The amount of remaining dextran at the surface of the particles was determined by direct titration of the particles. Typically, 50 mg of freeze-dried particles was dispersed in 10 g of distilled water. Two hundred microliters of the suspensions was added to the solution of anthrone in aqueous sulfuric acid. After 30 min at 80 °C, the suspensions were allowed to cool down to RT and were centrifuged at 20,000×*g* for 20 min. The clear supernatants were analyzed by UV spectroscopy at 625 nm. The calibration was obtained from suspensions of uncoated polystyrene nanoparticles in native dextran solutions.

Electrophoretic mobility (μe) was determined in NaCl solutions as a function of ionic strength. The measurements were performed on a Zetasizer NanoZ (Malvern Instruments, UK). Zeta potential ζ was calculated from the electrophoretic mobility using the modified Booth equation [32]. This equation allows the calculation of zeta potential for any k and a, where k^{-1} is the Debye Hückel length and a is the radius of the particles, whereas the classical Smoluchowsky and Hückel equations are only applicable under two limiting cases, i.e., $ka>100$ and $ka>0.1$. The electrokinetic layer thicknesses (δ_{el}) were calculated from the evolution of the zeta potential vs k [10, 33].

Colloidal properties of the particles

The colloid stability of styrene dispersion towards added electrolyte was assessed by turbidimetry [34]. Typically, 100 μl of dispersions was added to 3 ml of NaCl (from 1.10^{-4} to 4 M). The samples were allowed to stand for 40 min and their absorbance was measured over the range of 450–700 nm at 50-nm intervals. The slope n of the straight line log(optical density) vs log(wavelength) was taken as an indicator of particle size.

The stability of the latexes towards freeze-drying was assessed by particle size measurements. The freeze-dried samples were redispersed in distilled water before analysis.

Analysis of the in situ formed dextran derivatives

The average molecular weights were calculated from multi-angle light scattering experiments (Wyatt, Mini Dawn, Santa Barbara, CA) in 0.1 mol l^{-1} $NaNO_3$ or DMSO, coupled with a size exclusion chromatography (SEC) system.

NMR spectra are performed in deuterated DMSO on a Brücker spectrometer Avance 300.

The MALDI TOF MS used to acquire the mass spectra was a Voyager-DE STR (Applied Biosystems, Framingham, MA). This instrument was equipped with a nitrogen laser (wavelength 337 nm) to desorb and ionize the samples. The instrument was operated in linear and reflectron mode. The ions were accelerated to a final potential of 20 kV. The positive ions were detected in all cases. The spectra were the sum of 300 shots and an external mass calibration of mass analyzer was used (mixture of peptides from Sequazyme™ standards kit, Applied Biosystems, Framingham, MA). Samples were prepared by dissolving the dextran solutions in water at a concentration of 10 g l^{-1}. The matrix used for all experiments was 2,5 dihydroxybenzoic acid (DHB) purchased by Sigma-Aldrich (St. Louis, MO) and used directly without further purification. This solid matrix was dissolved in water with a 10 g l^{-1} concentration. A strong cation-exchange resin DOWEX 50W-X8, mesh size 200–400 (Supelco, Bellefonte, PA), was added to the matrix and sample solutions to decrease the salt quantity, which was shown to have a deleterious effect on MALD ionization [35]. Finally, 45 μl of matrix solution was mixed with 5 μl of the dextran solution, and 1 μl of the resulting mixture was deposited onto the MALDI target before insertion into the ion source chamber.

Results and discussion

Styrene emulsion polymerization in the presence of dextran

Styrene emulsion polymerizations were performed in the presence of different samples of native dextran (T6, T40 and T500) and initiated by KPS or AIBN. The polymer concentration in the aqueous phase (C in grams per liter) and the oil volume fraction (φ) were varied.

In the case of AIBN-initiated emulsion polymerization, the amount of coagulum reached about 50 wt.%, while the particle size remained above 1 μm. No control of particle size by the dextrane concentration was observed. Conversely, in the case of KPS-initiated polymerization, highly stable latexes were obtained. For a given dextran sample, it appeared that the key parameter to control the final particle size was the initial weight ratio α=[dextran]/[styrene] (Fig. 1).

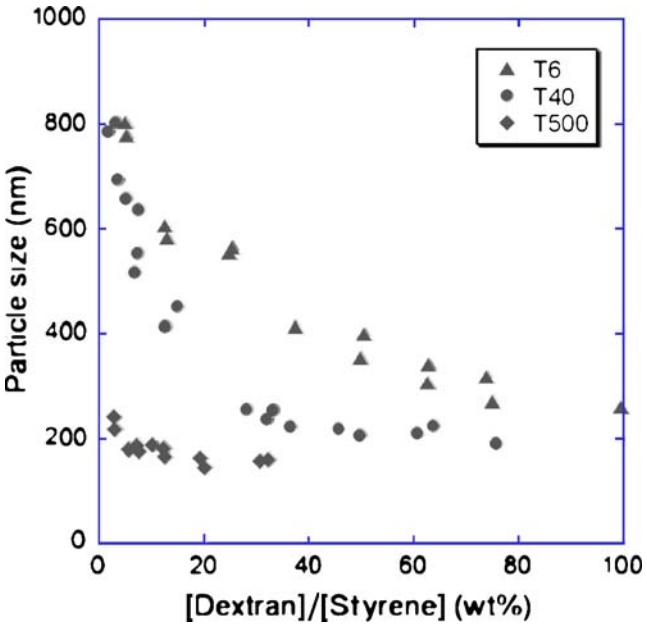

Fig. 1 Particle size as a function of [dextrane]/[styrene] mass ratio for the three dextran samples T6, T40, and T500, with average molar masses of 6,430, 40,000 and 480,000 g mol^{-1}, respectively

Up to a critical [dextran]/[styrene] ratio, particle size decreased and finally leveled off for the higher polysaccharide concentration. The standard deviation of size distribution decreased on the same time, as depicted on scanning electron microscopy pictures (Fig. 2) and highly monodisperse polystyrene nanoparticles were synthesized at high dextran concentration. Such a direct control of final particle size by the dextran concentration was never reported. More complex relationships were observed for still unclear reasons [19, 23].

The molar mass of the dextran had a great influence on final polystyrene particle size (Fig. 1). Smaller particles were obtained for the dextran T500, especially at low concentration. It seems that the dextran T500 is more efficient to stabilize the formed nanoparticles.

The presence of both dextran and KPS clearly gives rise to the formation of a stabilizing layer at the interface between polymeric particles and water. An empirical correlation is evidenced between dextran molar mass and stabilizing efficiency. More experiments are required to obtain more quantitative results.

Colloidal properties of the dextran-coated nanoparticles

The amount of dextran needed to stabilize the emulsion polymerization of styrene is relatively high. In the case of dextran T40, the plateau value of particle diameter was obtained for a [polysaccharide]/[styrene] ratio of about 40%. By comparison, in the case of amphiphilic derivatives of dextran, a [polysaccharide]/[styrene] ratio of only 5% is required [36]. Obviously, only a part of the native dextran is able to stabilize the emulsion polymerization of styrene. Indeed the amount of non-adsorbed polysaccharide remaining in the aqueous phase after polymerization was determined using the anthrone method (Fig. 3).

Results showed that only half of the polysaccharide was adsorbed on the particles after polymerization. Conversely, the amount of adsorbed amphiphilic dextran derivatives reached about 90% in the case of miniemulsion polymerization [36].

Γ, the amount of adsorbed dextran T40 (Fig. 3) regularly increased as the [polysaccharide]/[styrene] ratio increased. However, the polysaccharidic layer is not stable. After washing the particles via centrifugation and redispersion in distilled water to eliminate the non-adsorbed polysaccharide, the amount of remaining dextran at the surface of the particles was determined by direct titration of the particles. Γ decreased from about 10 to 3 mg m^{-2}. Further washing did not reduce Γ any more. When plotting the particle surface coverage (Γ, milligram per square meter) as a function of the concentration of non-adsorbed polymer remaining in the aqueous phase (C_{excess} in grams per liter), we get a curve having the shape of an adsorption isotherm (Fig. 3). Furthermore, the curve can be linearized using the Scatchard method [37, 38], and we get a maximum surface coverage equal to 2.5 mg m^{-2}, which agrees with the

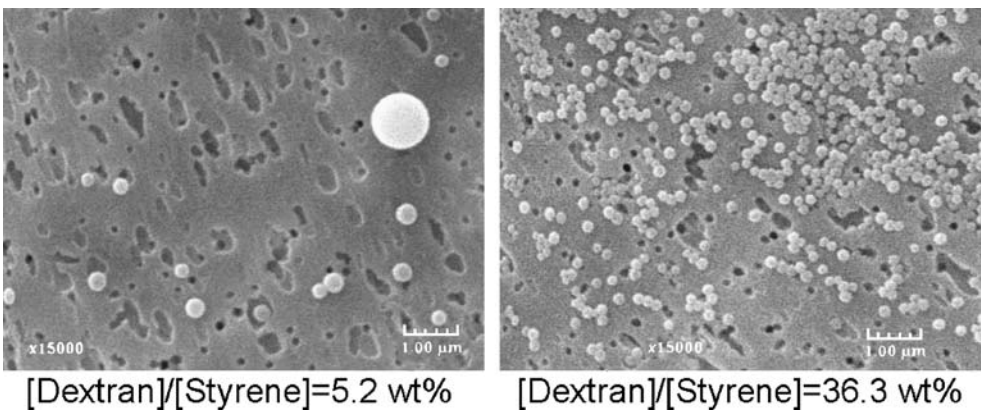

Fig. 2 Scanning electron microscopy pictures of polystyrene nanoparticles prepared by emulsion polymerization in the presence of dextran T40 at varying [dextrane]/[styrene] ratios

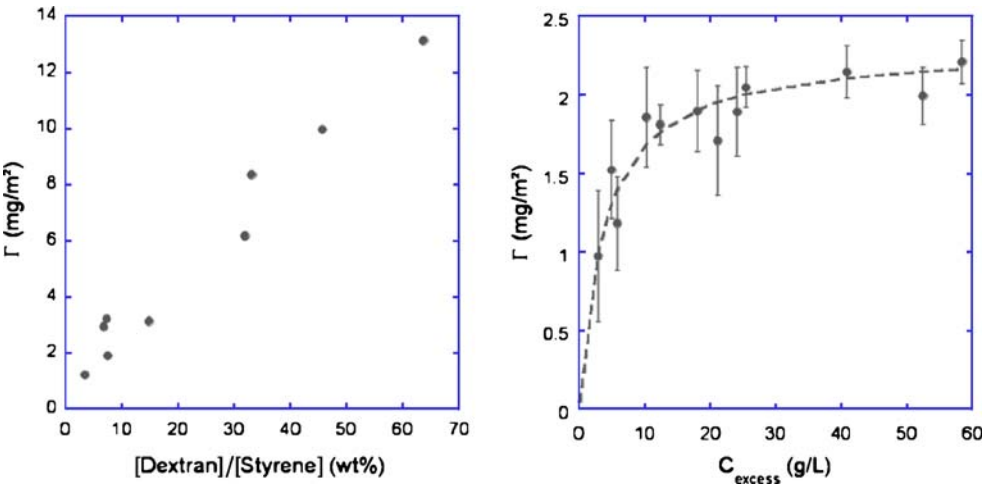

Fig. 3 Surface coverage of particles by dextran T40 as a function of polymer concentration remaining in the aqueous phase. *Left* Surface coverage of particles directly after emulsion polymerization. *Right* Surface coverage of the same particles after extensively washing. The *line* is a curve fitting made by using the Scatchard equation

experimental results (Fig. 3). These results are consistent with the scarce values present in the literature [10, 19].

The variation of the amount of adsorbed dextran at the surface of the particles with the molecular weight of the polysaccharide remained below the uncertainty of the methods.

Electrokinetic layer thickness was evaluated via Zeta potential measurements at increasing salt concentrations, using the Eversole Boardman equation [5] (Fig. 4).

A sharp increase of the polysaccharidic layer thickness was observed at low [dextrane]/[styrene] ratio. For α higher than 20 wt.%, the electrokinetic layer thickness only slightly increased with dextran concentration in the aqueous phase. The values obtained are consistent with the only one reported in the literature [10].

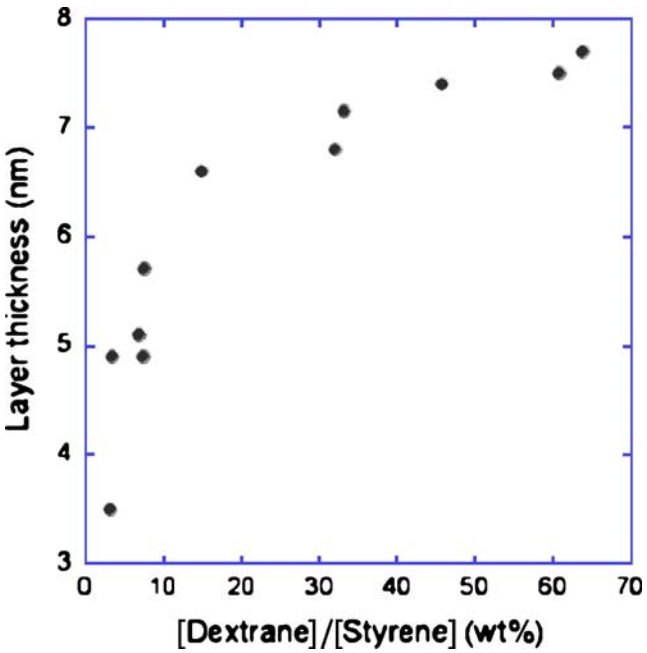

Fig. 4 Variation of the electrokinetic layer at the surface of the particles as a function of the initial dextran T40 concentration

This neutral hydrophilic polymeric layer provided good colloidal stability to the polystyrene nanoparticles. The colloidal stability of latex suspensions in the presence of added electrolyte was assessed by turbidimetry [34]. Above 0.1 M NaCl, bare polystyrene nanoparticles are no longer stable because of the screening of the surface charges coming from the initiator by salt ions. Therefore, flocculation due to Van der Waals attraction occurred when the salt concentration increased. In contrast, no flocculation was observed at NaCl concentration up to 4 M for the dextran-coated polystyrene nanoparticles, as a result of steric stabilization by osmotic and elastic repulsion potentials.

The effect of the dextran layer on the stability of particles during freeze-drying was also examined. To avoid aggregation of particles, latexes obtained with low molecular weight surfactants have to be freeze-dried with a cryoprotectant such as glucose and sucrose trehalose [39–42]. In our case, no cryoprotectant was required and particles could easily be redispersed in water after freeze-drying. Particle size before and after freeze drying were about the same (Table 2).

Structure of the in situ formed dextran derivatives

The formation of polystyrene nanoparticles with a permanent dextran layer is only possible if the polysaccharide is chemically modified because native dextran do not adsorb onto polystyrene nanoparticles. In this study, chemical modification of dextran at least began in the aqueous phase. Indeed, when AIBN, an oil soluble initiator is used, no control of the emulsion polymerization process was observed, meaning that the chemical modification of dextran did not occur at all. Thus, in the case of KPS-initiated polymerization, dextran probably first reacted with the water-soluble initiator and the fraction of monomer soluble in water. As already mentioned, dextran undergoes different reactions (chain

Table 2 Particle sizes of nanoparticles obtained by emulsion polymerization of styrene in the presence of dextran T40 before and after freeze drying

[dextran T40]/ [styrene] (wt.%)	Particle size before freeze-drying (nm)	Particle size after freeze-drying (nm)
1.7	785	*
3.5	618	*
6.9	607	642
7.4	533	553
12.6	452	457
14.9	376	378
16.4	237	241
28.2	216	218
45.8	219	221
49.8	206	204
60.8	210	215
75.8	191	190

An asterisk within a cell denotes non-redispersable nanoparticles.

scission, grafting process) in the presence of radicals (Scheme 1, rewritten from [43]). Thus, depending on the reaction pathway followed, either block copolymers or graft copolymers are likely to be formed.

To identify the nature of the dextran derivatives formed, samples were removed at frequent intervals and quenched by addition of hydroquinone followed by rapid cooling in an ice/water mixture. The samples were purified by dialysis against ethanol/water 80/20 mixtures then water, and finally freeze-dried.

No chain scissions of the polysaccharide occurred during all the processes, as proved by SEC analysis of the polymers formed. Indeed, the molecular weight of the polysaccharides remained more or less constant throughout the reaction. In view of the SEC analysis, the formation of block copolymers is unlikely, as chain scission is required before their synthesis (see Scheme 1). Therefore, we expect the in situ-formed derivatives to be a graft copolymer.

^{1}H NMR spectra of the quenched samples were recorded in deuterated DMSO. The lines corresponding to the glucose units of the polysaccharidic backbone remained unchanged. However, weak lines appeared with chemical shifts corresponding to aromatic protons. These results suggest that the major part of the dextran is not modified during the emulsion polymerization. This is consistent with the surface coverage measurements. Indeed, the major part of the dextran is not adsorbed or could be easily washed from the particles.

The lines in the spectral region of aromatic functions could be due to small grafted units and free polystyrene. In

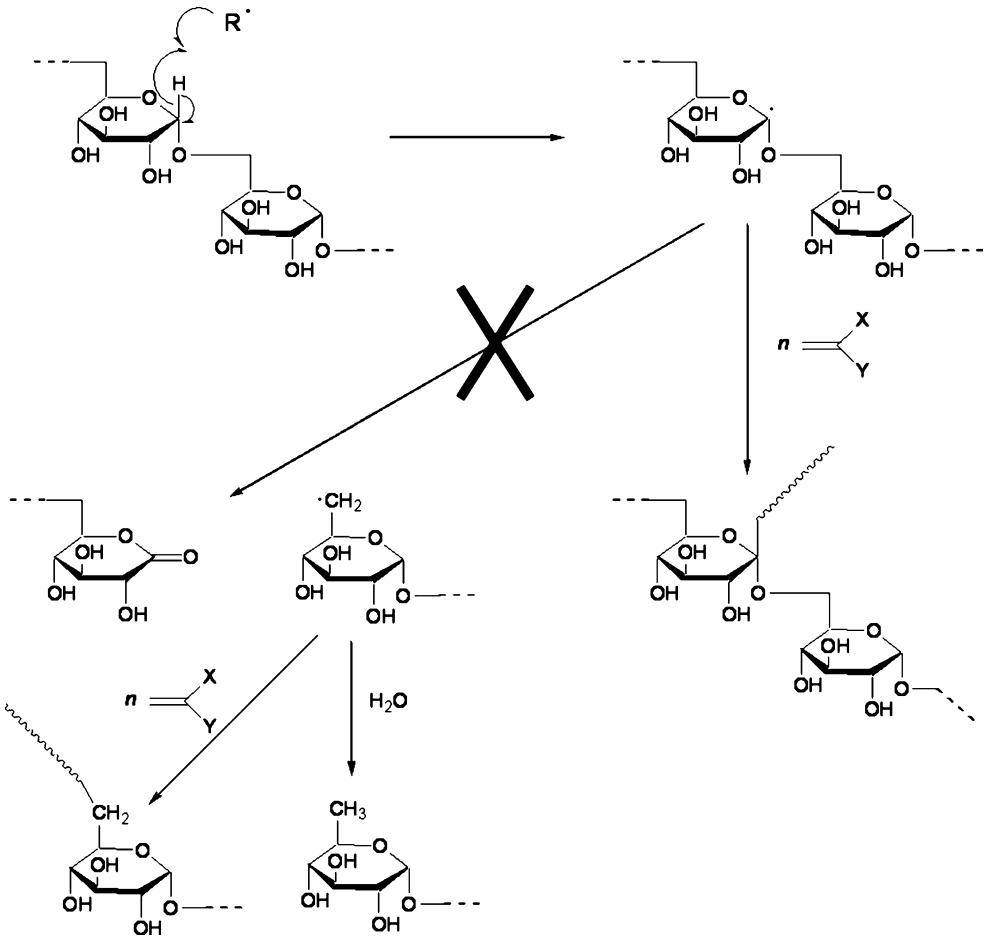

Scheme 1 Mechanisms of formation of amphiphilic dextran during the emulsion radical polymerization initiated by KPS

order to settle, proton NMR spectra of dextran-coated nanoparticles suspended in deuterated DMSO were recorded (Fig. 5). This solvent totally dissolves the dextran outer layer, but only swells the polystyrene core. For comparison, the proton NMR spectra of styrene and bare polystyrene nanoparticles recorded in the same conditions are given.

The more reliable results are concentrated in the spectral region pertaining to the aromatic groups. Indeed, the chemical shifts of the lines pertaining to the glucose units are only weakly affected by the substitution of their OH groups [44]. Therefore, the only spectral data from the aromatic region is discussed in the following. Besides the broad lines due to the polystyrene main chains, weak lines are visible between 8.4 and 7.3 ppm. These lines are well resolved and narrow and may correspond to low molecular weight species (oligomers). The lines of the remaining monomer were unambiguously assigned by comparison with the NMR spectrum of styrene. When comparing the spectra of bare nanoparticles and dextran-coated nanoparticles, the lines in the 7.4- to 8.4-ppm region are totally different. This suggests that different species are formed in the two cases. The only difference came from the stabilizers used, SDS in one case and dextran in the other; this suggests that the dextran reacted with the polystyrene to form a copolymer. These lines may thus be assigned to the formation of small polystyrene chains grafted onto the dextran backbone.

Finally, MALDI TOF mass spectrometry analysis was performed on dextran-T6 coated polystyrene nanoparticles. To optimize the conditions, the positive-ion MALDI mass spectrum of dextran T6 was first measured, on the basis of former studies [45–49] and is reported in Fig. 6.

The peak-to-peak mass difference is 162 mass units, confirming that the repeat unit is $C_6H_{10}O_5$. The sodium and potassium cationized dextran species with expected end groups (i.e., H and OH groups) are well-observed in the expended zone of a spectrum acquired in reflector mode for a better resolution. However, the molecular weight measured is well below the values measured by size exclusion chromatography, meaning that only partial desorption of the dextran from the matrix was obtained (the so-called molar mass discrimination effect) [50–54].

The positive-ion MALDI mass spectrum of dextran-coated nanoparticles is reported in Fig. 7.

The molecular weight distribution is centered at 1,260 g mol^{-1}, which is totally different from the originated dextran. Once more, this molecular weight is below the expected one, suggesting a partial desorption of the polymer. The peak-to-peak mass difference is 58 mass units, which corresponds to 162 (glucose unit) minus 104 (styrene unit), the difference usually observed in the copolymer studies. These results thus confirm the formation of a dextran–styrene copolymer. However, three peak-to-peak differences of 58, 104, and 162 mass units, respectively, were expected for a dextran–styrene copolymer. This may be due to the only partial desorption according to the nature of copolymer end groups.

Unfortunately, we did not succeed in purifying the formed copolymers for further characterizations. Indeed, such a copolymer with a hydrophilic backbone and hydrophobic grafted chains might exhibit amphiphilic properties, which would explain the experimental results. The trickiest fact is the influence of the molar masses of the dextran used during the emulsion polymerization of styrene onto the final particle size. The variation of the amount of adsorbed dextran at the surface of the particles with the molecular weight of the polysaccharide remained below the uncertainty of the methods. Furthermore, we do not expect the reactivity of the dextran to depend on the average molar mass of the polysaccharide. However, we did not succeed

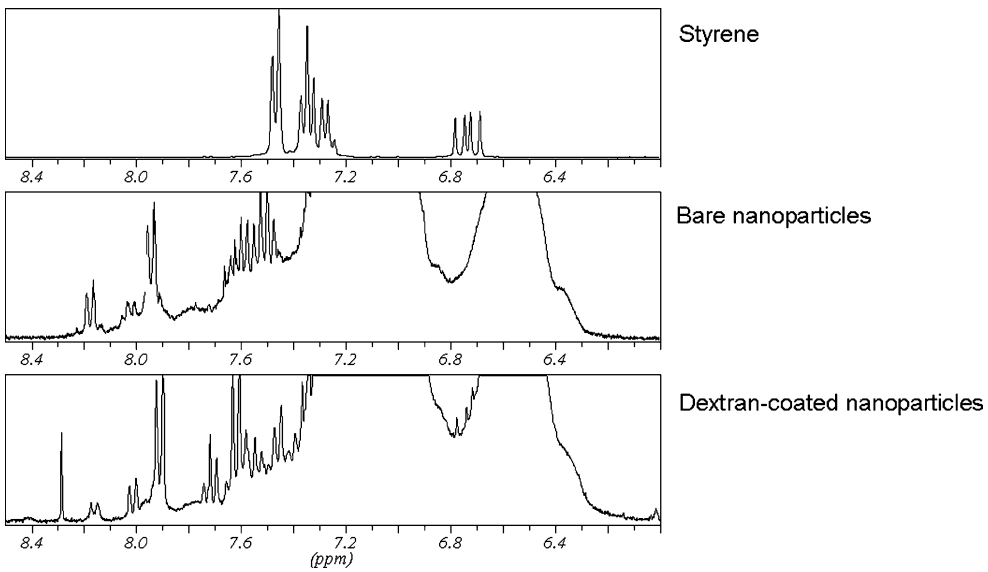

Fig. 5 ^{1}H NMR spectra of styrene (*top*), bare nanoparticles (*center*) and dextran-coated nanoparticles (*bottom*) in deuterated DMSO

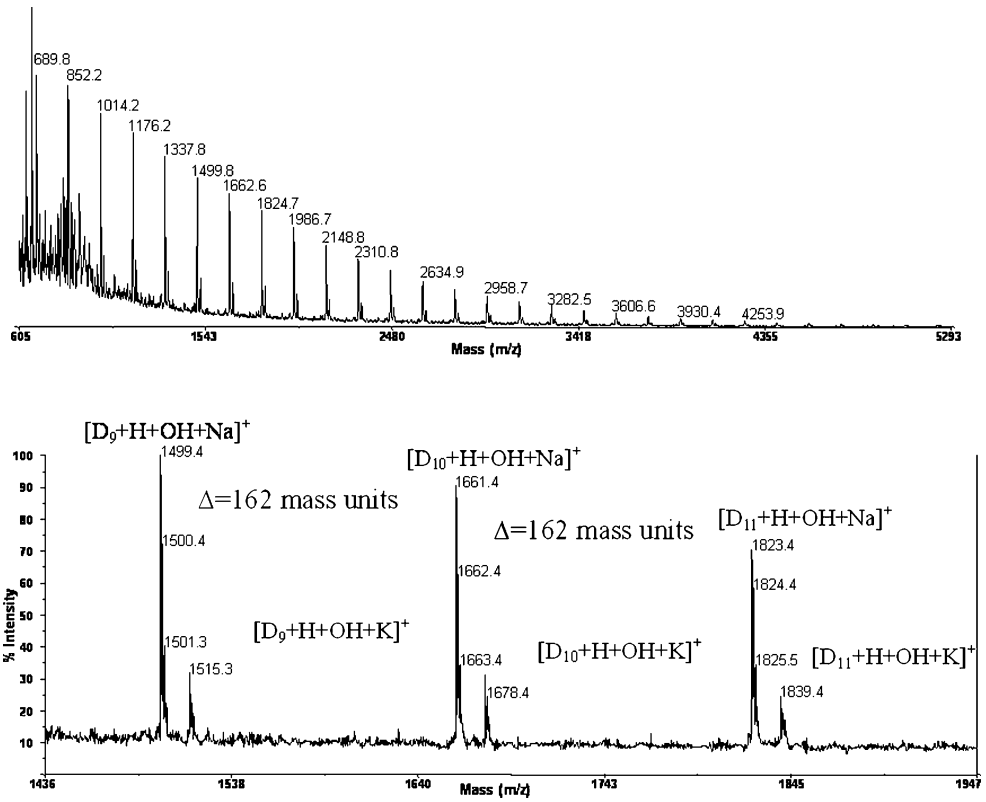

Fig. 6 Positive-ion MALDI-TOF mass spectrum of dextran T6 with DHB matrix (in linear mode). The *lower part* shows an expanded zone of spectrum (between m/z 1,436 and 1,947) acquired in reflector mode (higher resolution)

in the analysis of the dextran derivatives formed in the presence of Dextran T40 and T500 as MALDI-TOF spectroscopy is not able to analyze high molecular weight polysaccharides.

Two parameters have to be taken into consideration. For a given [dextran]/[styrene] weight ratio, the number of grafted unit per macromolecular chain will depend on the molecular weight of the polysaccharide. The higher the

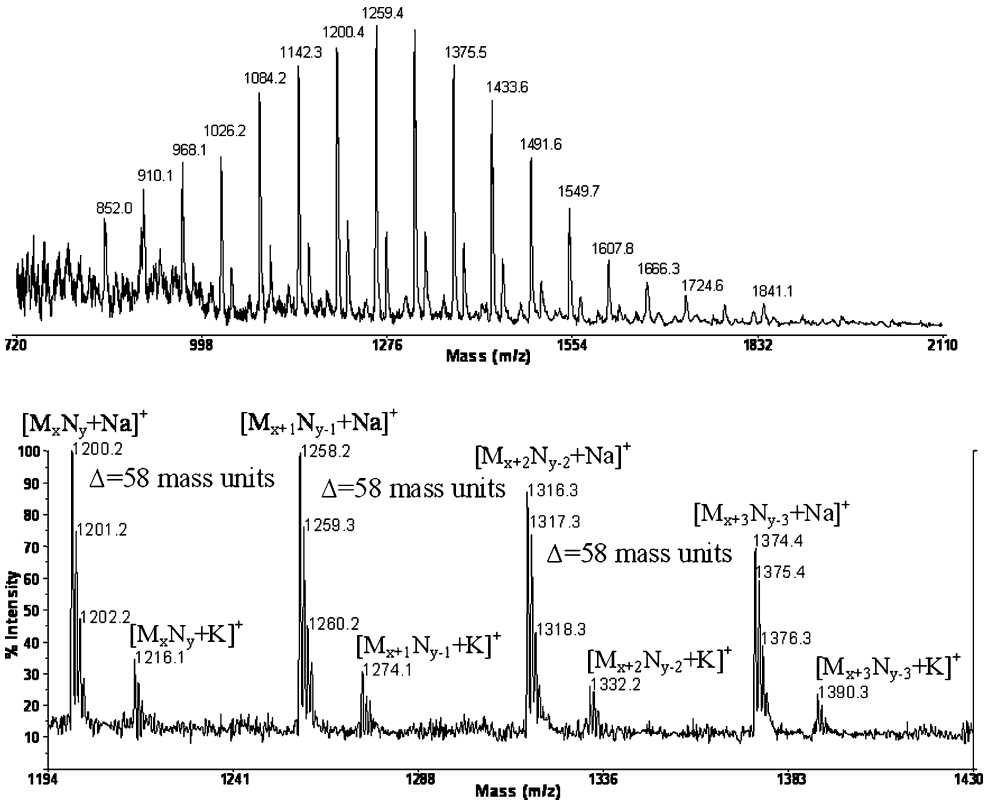

Fig. 7 The positive-ion MALDI mass spectrum of dextran-coated nanoparticles

molecular weight, the higher the number of grafted unit per chain. This means that the number of anchoring points onto the surface of the nanoparticles increases with the molecular weight of dextran, which could confer a greater stability to the nanoparticles. The other important point might be the viscosity of the aqueous phase. Indeed, the intrinsic viscosity (η) of dextran T40 and T500 in water at 25 °C are 20 and 52 ml g^{-1}, respectively [55]. However, further experiments are required to elucidate this point.

Conclusions

In the foregoing, the preparation of polysaccharide-coated nanoparticles by direct emulsion polymerization of styrene in the presence of native dextran is carefully described. In spite of the lack of surface-active properties of native dextran, stable latexes with very low amount of coagulate were obtained. Particle size decreased with dextran concentration and molecular weight.

The amount of permanently adsorbed dextran was determined by direct titration of the polysaccharide present on the surface of the nanoparticles. A maximum value of 2.5 mg m^{-2} was found. Zeta-potential measurements allowed us to estimate the thickness of the hydrophilic layer, which regularly increased with dextran aqueous concentration. The dextran-coated polystyrene nanoparticles were stable in concentrated NaCl solutions and could be redispersed after freeze-drying.

The nature of the in situ formed dextran derivatives was studied by NMR and MALDI-TOF mass spectrometry studies. Graft copolymers are supposed to be formed.

Acknowledgments The authors thank F. Delolme (SCA/CNRS, Solaize, France) for the use of the MALDI-TOF mass spectrometer and for fruitful discussions. The assistance of M.-C. Grassiot in emulsion polymerization and particle analysis is gratefully acknowledged.

References

1. Fournier C, Leonard M, Coq-Leonard IL, Dellacherie E (1995) Langmuir 11:2344
2. Fournier C, Leonard M, Dellacherie E, Chikhi M, Hommel H, Legrand AP (1998) J Colloid Interface Sci 198:27
3. Rouzes C, Gref R, Leonard M, Delgado ADS, Dellacherie E (2000) J Biomed Mater Res 50:557
4. Rouzes C, Leonard M, Durand A, Dellacherie E (2003) Colloid Surf B Biointerfaces 32:125
5. Delgado ADS, Leonard M, Dellacherie M (2000) J Biomater Sci Polym Ed 11:1395
6. Durand A, Marie E, Rotureau E, Leonard M, Dellacherie M (2004) Langmuir 20:6956
7. Rotureau E, Marie E, Leonard M, Dellacherie E, Camesano TA, Durand A (2006) Colloids Surf A (in press)
8. Imbert P, Sadtler VM, Dellacherie E (2002) Colloids Surf A Physicochem Eng Asp 211:157
9. Sadtler VM, Imbert P, Dellacherie E (2002) J Colloid Interface Sci 254:355
10. C Rouzes, Durand A, Leonard M, Dellacherie E (2002) J Colloid Interface Sci 253:217
11. Rotureau E, Leonard M, Dellacherie E, Durand A (2004) Phys Chem Chem Phys 6:1430
12. Passinari C, Barratt G, Devissaguet J-P, Labarre D (1998) Pharm Res 15:1046
13. Passinari C, Ferrarini L, Barratt G, Devissaguet JP, Labarre D (1999) J Biomater Sci Polym Ed 10:47
14. Zhang LM, Chen DQ (2001) Starch/Stärke 53:311
15. Chauvierre C, Labarre D, Couvreur P, Vauthier C (2003) Pharm Res 20:1786
16. Chauvierre C, Labarre D, Couvreur P, Vauthier C (2003) Macromolecules 36:6018
17. Chauvierre C, Vauthier C, Labarre D, Hommel H (2004) Colloid Polym Sci 282:1016
18. Gritskova IA, Vakekeva IF, Grzywa-Niksinska I, Legocki M, Basyreva L, Grzywa E (1996) Polimery 41:503
19. Chern CS, Lee CK, Tsai YJ (1997) Colloid Polym Sci 275:841
20. Chern CS, Lee CK, Tsai YJ, Ho CC (1998) Colloid Polym Sci 276:427
21. Chern CS, Lee CK, Tsai YJ (1999) Colloid Polym Sci 277:528
22. Jaulin N, Appel M, Passinari C, Baratt G, Labarre D (2000) J Drug Target 8:165
23. Men'shikova AY, Evseeva TG, Chekina NA, Ivanchev SS (2001) Russ J Appl Chem 74:489
24. Men'shikova AY, Evseeva TG, Chekina NA, Skurkis YO, Ivanchev SS (2003) Polym Sci Ser A 45:380
25. Ferguson CJ, Hughes RJ, Pham BTT, Hawkett BS, Gilbert RG, Serelis AK, Such CH (2002) Macromolecules 35:9243
26. Ferguson CJ, Hughes RJ, Nguyen D, Pham BTT, Gilbert RG, Serelis AK, Such CH, Hawkett BS (2005) Macromolecules 38:2191
27. Monteiro MJ, Adamy MM, Leeuwen BJ, van Herk AM, Destarac M (2005) Macromolecules
28. Fréal-Saison S, Magnet S, Save M, Charleux B (2005) Polymer Preprints 46:128
29. Delaittre G, Nicolas J, Lefay C, Save M, Charleux B (2005) Chem Commun 5:614
30. Nicolas J, Charleux B, Guerret O, Magnet S (2005) Macromolecules 38:9963
31. Scott TA, Melvin EH (1953) Anal Chem 25
32. Deshiikan SR, Papadopoulos KD (1998) Colloid Polym Sci 276:117
33. Delgado ADS, Léonard M, Dellacherie E (2001) Langmuir 17:4386
34. Meadows J, Williams PA, Garvey MJ, Harrop R (1992) J Colloid Interface Sci 148:160
35. Danis PO, Karr DE, Mayer F, Holle A, Watson CH (1992) Org Mass Spectrom 27:843
36. Marie E, Landfester K, Antonietti M (2002) Biomacromolecules 3:475
37. Scatchard G (1949) Ann N Y Acad Sci 51:660
38. Klotz IM, Hunston D (1971) Biochemistry 10:3065
39. Chateigner SD, Cavé G, Fessi H, Devissaguet J-P, Puisieux F (1996) Drug Dev Res 38:116
40. Cavalli R, Caputo O, Carlotti ME, Trotta M, Scarnecchia C, Gasco MR (1997) Int J Pharm 148:47
41. Schaffazick SR, Pohlmann AR, Dalla-Costa T, Guterres SS (2003) Eur J Pharm Biopharm 56:501
42. Oh KS, Lee KE, Han SS, Cho SH, Kim D, Yuk SH (2005) Biomacromolecules 6:1062
43. Annable T, Gray I, Lovell PA, Richards SN, Satgurnathan G (2004) Prog Colloid & Polym Sci 124:159

44. Nouvel C, Ydens I, Degée P, Dubois P, Dellacherie E, Six J-L (2002) Polymer 43:735
45. Chan PK, Chan TWD (2000) Rapid Commun Mass Spectrom 14:1841
46. Chan TWD, Tang KY (2003) Rapid Commun Mass Spectrom 17:887
47. Malvagna P, Impallomeni G, Cozzolino R, Spina E, Garozzo D (2002) Rapid Commun Mass Spectrom 16:1599
48. Bashir S, Derrick PJ, Critchley P, Gates PJ, Staunton J (2003) Eur J Mass Spectrom 9:61
49. Bashir S, Giannakopulos AE, Derrick PJ, Critchley P, Bottrill A, Padley HD (2004) Eur J Mass Spectrom 10:109
50. Martin K, Spickermann J, Räder HJ, Müllen K (1996) Rapid Commun Mass Spectrom 10:1471
51. Spickermann J, Martin K, Räder HJ, Müllen K (1996) Eur J Mass Spectrom 2:161
52. Axelsson J, Scrivener E, Haddleton DM, Derrick PJ (1996) Macromolecules 29:8875
53. Zammit MD, Davis TP, Haddleton DM, Suddaby KG (1997) Macromolecules 30:1915
54. Montaudo G, Montaudo MS, Puglisi C, Samperi F (1995) Rapid Commun Mass Spectrom 9:453
55. Rotureau E, Dellacherie E, Durand A (2006) Eur Polym J 42: 1086